Imaging Features of Prostate Sarcoma: A Case Report

Federica Masino[1], Laura Eusebi[2], Manuela Montatore[1], Giuseppe Maria Andrea D'Arma[1], Giuseppe Sortino[3], Lucia Pitoni[3], Alessandra Filosa[4], Giuseppe Guglielmi[1,5,6]

[1] Department of Clinical and Experimental Medicine, Foggia University School of Medicine, Foggia, Italy;
[2] Radiology Unit, "Carlo Urbani" Hospital, Jesi, Italy;
[3] Urology Unit, "Carlo Urbani" Hospital, Jesi, Italy;
[4] Anatomic Pathology Unit, "Carlo Urbani" Hospital, Jesi, Italy;
[5] Radiology Unit, "Dimiccoli" Hospital, Barletta, Italy;
[6] Radiology Unit, "IRCCS Casa Sollievo della Sofferenza" Hospital, San Giovanni Rotondo, Italy

Received June 23, 2024; Accepted May 12, 2025.

Key words: Prostate sarcoma – Prostate tumour – Imaging – Radiology – MRI

Abstract: A 54-year-old man presented to our clinic complaining of painful ejaculation. The patient underwent various imaging modalities, including ultrasound, transrectal ultrasound, prostate magnetic resonance imaging and positron emission tomography/computed tomography that detected a voluminous mass originating from the prostate. Histological examination diagnosed a prostate sarcoma, a rare mesenchymal tumour. This case offers an opportunity to evaluate a rare subtype of prostate cancer and to describe its main imaging features with an educational approach.

Mailing Address: Prof. Giuseppe Guglielmi, MD., Department of Clinical and Experimental Medicine, Foggia University School of Medicine, Viale L. Pinto 1, 71121, Foggia, Italy; e-mail: giuseppe.guglielmi@unifg.it

https://doi.org/10.14712/23362936.2025.16

Introduction

Prostate sarcoma is a rare malignancy arising from the mesenchymal tissues of the prostate gland. It accounts for about 0.1% of all prostate malignancies and typically arises in adults with an average age of 50 to 60 years (Ehat et al., 2023). The exact aetiology of prostate sarcoma remains obscure, although some cases have been associated with genetic predispositions, prior radiation therapy, and exposure to certain chemicals (Girling et al., 2007).

Patients with prostate sarcoma often present with nonspecific symptoms, such as urinary frequency, urgency, haematuria, and obstructive voiding symptoms. In advanced stages, patients may experience pelvic pain, lower back pain, weight loss, and constitutional symptoms indicative of systemic involvement. The insidious onset and lack of specific symptoms often lead to delayed diagnosis and advanced disease at presentation (Jaouani et al., 2023).

No reliable tumour markers for prostate sarcoma have been identified, with serum prostate-specific antigen (PSA) values usually normal due to the non-epithelial origin of these tumours (Arham et al., 2024).

Diagnosis of prostate sarcoma relies on a combination of clinical evaluation, imaging studies, and histopathological analysis. Transrectal ultrasound (TRUS), magnetic resonance imaging (MRI), and computed tomography (CT) scans are commonly employed to assess the extent of local invasion and detect distant metastases. Definitive diagnosis is established through prostate biopsy, with histopathological examination revealing characteristic features of sarcomatous tissue (Andreou et al., 2013).

Prostate sarcomas encompass a diverse group of histological subtypes. In children, the most common tumour type is a prostatic rhabdomyosarcoma (42% all prostatic sarcomas). In adults, leiomyosarcomas are most common (25% of all cases). Other types of prostatic sarcomas include sarcomatoid carcinoma; malignant fibrous histiocytoma; phyllodes tumour (also known as cysto-sarcoma phyllodes); undifferentiated stromal sarcoma of the prostate. Histological examination typically reveals spindle-shaped or pleomorphic cells with varying degrees of differentiation. Immunohistochemical analysis plays a crucial role in confirming the diagnosis and identifying specific markers associated with different subtypes (Andreou et al., 2013; Phuong et al., 2023).

Prostate sarcoma is associated with a poor prognosis, with five-year survival rates ranging from 20 to 40% depending on the histological subtype and stage of disease at presentation. Factors associated with worse outcomes include advanced age, large tumour size, high-grade histology, presence of metastases, and incomplete surgical resection. Despite aggressive multimodal therapy, local recurrence and distant metastases frequently occur, contributing to significant morbidity and mortality (Qin et al., 2023).

Treatment typically involves a multidisciplinary approach, including urologists, oncologists, radiotherapist, and radiologists. Surgical resection with wide margins remains the cornerstone of treatment for localized disease, although achieving negative surgical margins can be challenging given the propensity for local invasion. Adjuvant radiation therapy may be employed to improve local control and reduce the risk of local recurrence (Hodotsuka et al., 2023).

Case report

A 54-year-old male patient presented to our department complaining of painful ejaculation for a couple of years. He did not report haematuria, and he had no significant past medical history. Laboratory tests including PSA were within normal ranges. A trans-abdominal prostate ultrasound (US) was performed (Figure 1).

The US findings necessitated a specialist urological evaluation. The patient underwent a transrectal US (TRUS) examination (Figure 2).

A prostate MRI (1.5T) performed before and after contrast administration was necessary to better characterize the mass, evaluate its relationships with surrounding structures and exclude their infiltrations. The protocol included multiplanar T1-weighted, T2-weighted, diffusion-weighted imaging (DWI) with apparent diffusion coefficient (ADC) mapping, 3D chemical shift imaging (CSI) sequences (Figures 3–5).

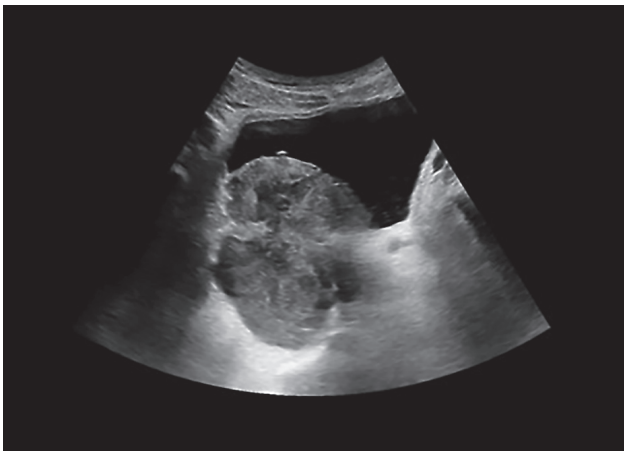

Figure 1: Prostate ultrasound image showing a prostate significantly increased in size (about 7 cm) due to the presence of a voluminous mass in the apical area, with mixed echogenicity, which imprinted and compressed the posterior bladder wall.

Prague Medical Report / Vol. 126 (2025) No. 2, p. 96–102

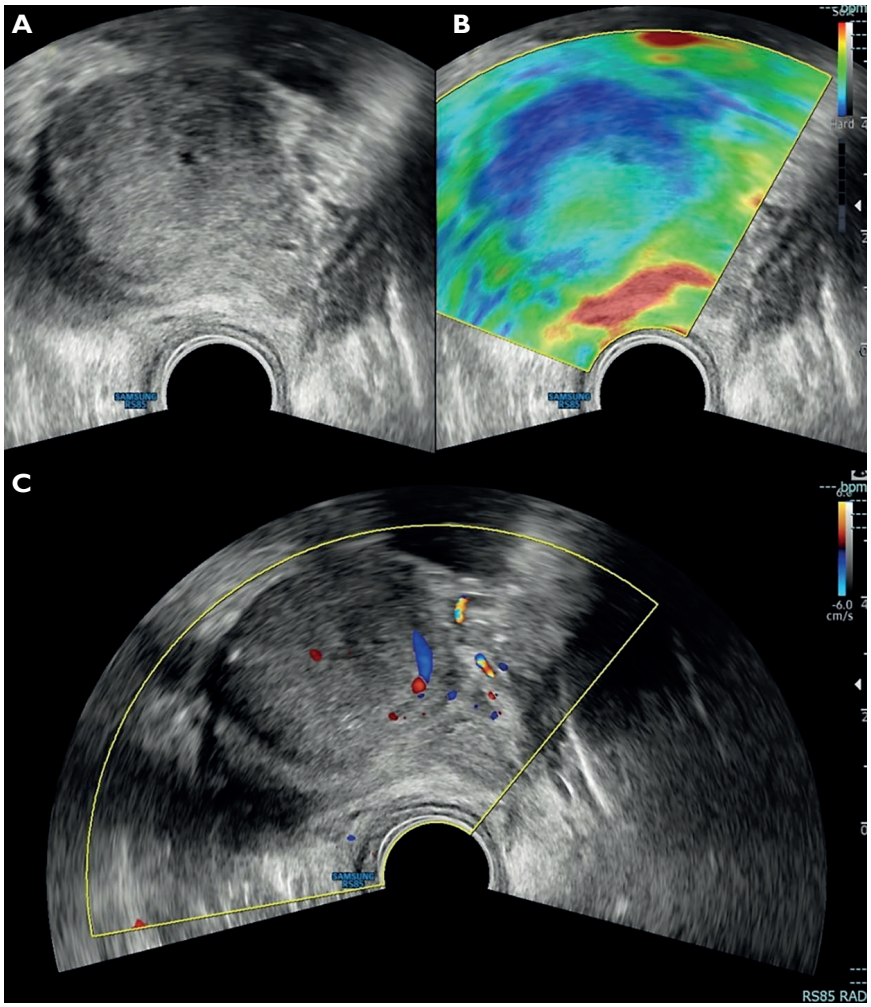

Figure 2: (A–C) Transrectal ultrasound confirmed the presence of a voluminous prostatic mass (A), with solid component showing intense blue colour on elastographic evaluation (B) and intralesional vascularization on colour Doppler evaluation (C), highly indicative of malignancy.

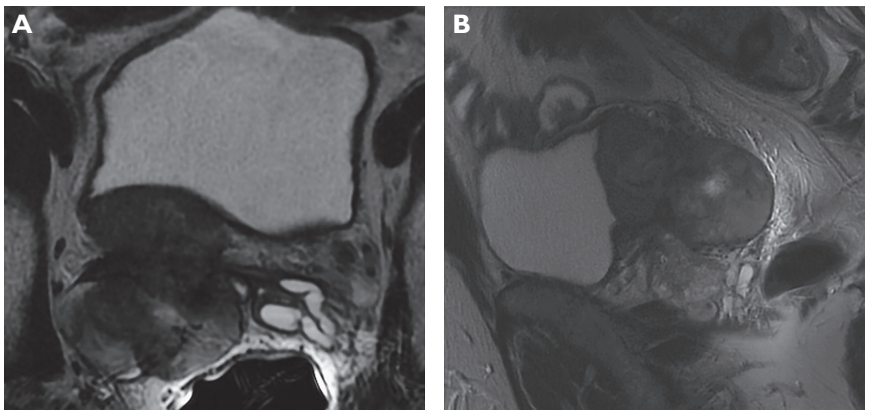

Figure 3: Axial (A) and sagittal (B) magnetic resonance imaging T2-w sequences showed a well-demarcated, heterogeneous lesion, mainly hypointense, arising from the central part of the apex and responsible of bladder compression.

The MRI examination findings revealed a heterogeneous mass, with an estimated diameter of 8×7×6 cm, arising from the prostate apex causing bladder compression, without clear infiltrative aspects. A more in-depth evaluation was requested with biopsy. The histological examination diagnosed a high-grade pleomorphic spindle cell malignant mesenchymal neoplasm, showing morphological and immunophenotypic characteristics (smooth muscle actin + multifocal; desmin –; caldesmon –;

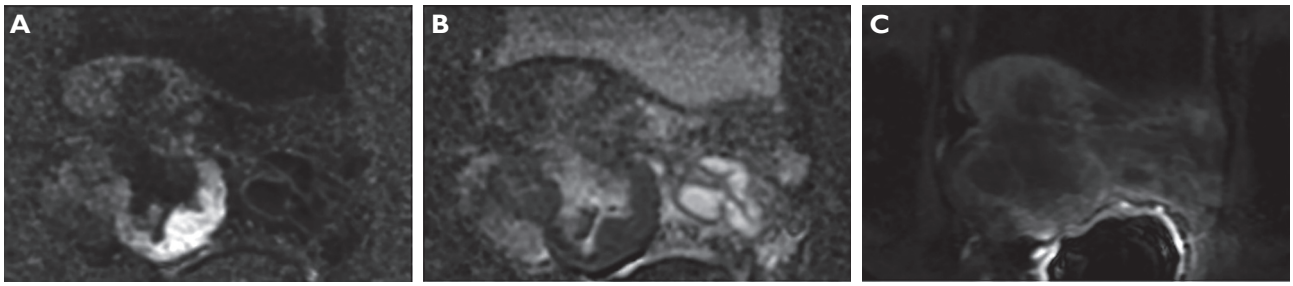

Figure 4: 1.5 magnetic resonance imaging: axial diffusion weighted imaging (A) and apparent diffusion coefficient map (B) image showed the presence of areas of diffusive restriction; axial post-contrast (C) image showed a peripherical enhancement surrounding the necrotic/colliquative central areas.

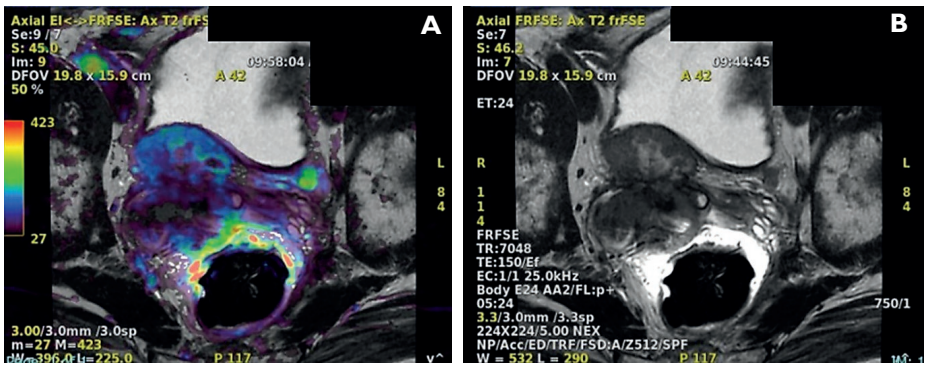

Figure 5: 3D-CSI 1.5 magnetic resonance imaging: coloured parametric maps (A) superimposed to T2-weighted image (B).

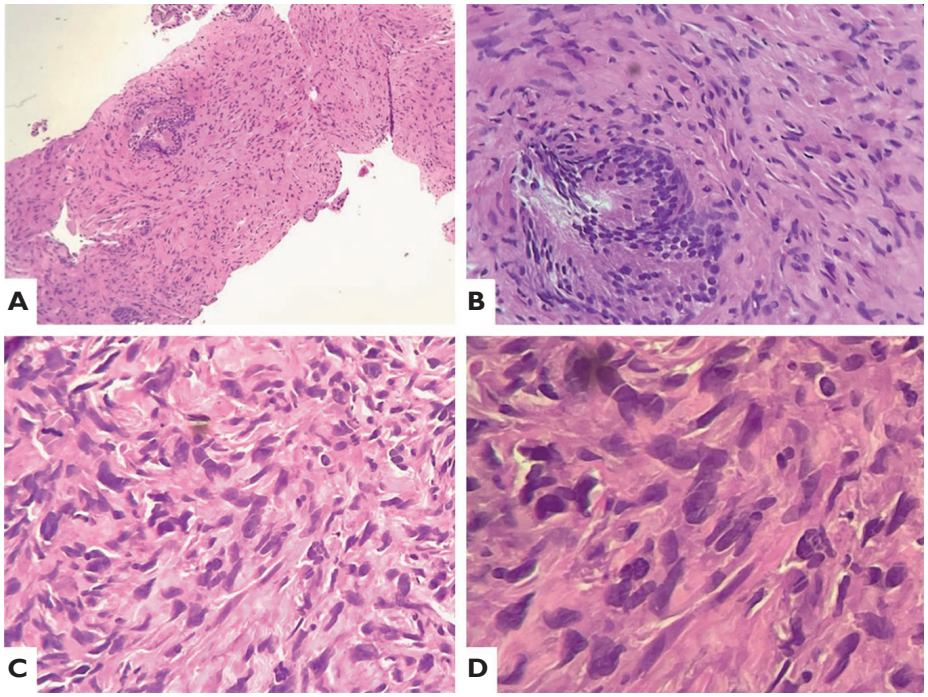

Figure 6: Proliferation of stromal cells that surrounds normal prostatic glands without destroying them (A, B). The proliferation is composed of fused and pleomorphic mesenchymal cells with areas of necrosis (not shown) with evident mitotic activity (C, D).

myogenin –; MDM2 –; H3K27me expression preserved; S100 –; cytokeratin MNF116 –) were consistent with the diagnosis of undifferentiated pleomorphic sarcoma, G3 according to French Federation of Cancer Centres Sarcoma Group (FNCLCC), which confirmed the presence of prostate sarcoma (Figure 6).

The patient underwent a positron emission tomography (PET)/CT with 18 F-FDG in order to exclude the presence of metastasis: the investigation

Prague Medical Report / Vol. 126 (2025) No. 2, p. 96–102

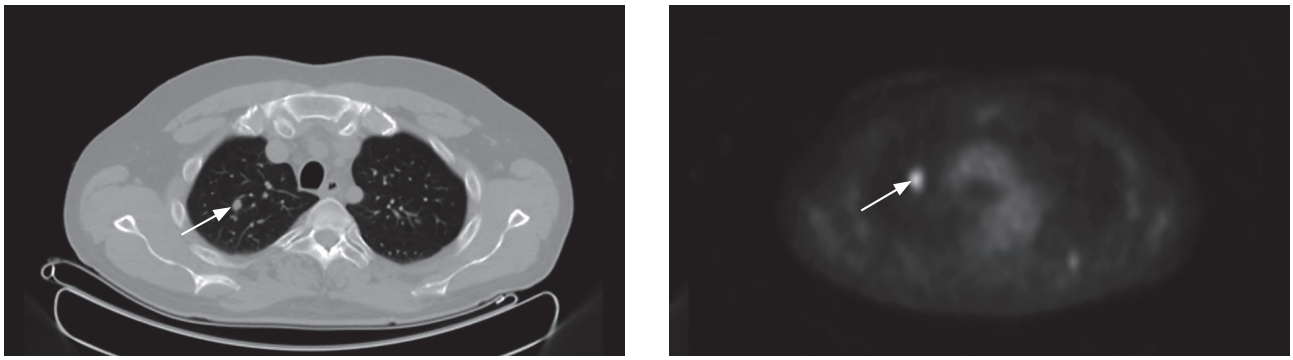

Figure 7: Axial thorax positron emission tomography/computed tomography image showing a pulmonary nodule (arrow) in the apical segment of the right upper lobe with hyper uptake of the 18 F-FDG, referable to secondaries.

revealed the presence of multiple and ubiquitous nodular lesions in both lung fields that showed hyper uptake of the radiotracer (Figure 7).

Treatment and patient management required a multidisciplinary approach and involved a combination of surgery to obtain clear margins, radiation therapy to control local extension, and chemotherapy to address systemic risks. However, imaging at six months revealed progression of lung metastases, prompting a change in the chemotherapy regimen. Regular follow-up with MRI and PET/CT continues to monitor disease status.

Discussion

Imaging techniques play a pivotal role in the detection, characterization, and staging of prostate sarcoma, aiding clinicians in making informed decisions regarding treatment strategies and patient care. Several imaging modalities are used in the global assessment of the neoplasm, each offering unique advantages and limitations (Andreou et al., 2013) (Table 1).

Imaging findings of prostate sarcoma may vary depending on the histologic subtype and stage of the disease. However, typically, prostate sarcoma presents as a heterogeneous mass within the prostate gland, often with irregular margins and areas of necrosis or haemorrhage. Prostate sarcomas generally are large at the time of diagnosis, with an average size of about 8 cm. Tumour shape varies from well-defined, roundish or lobular masses to irregular, ill-defined lesions (Luo et al., 2024).

In the reported case, the patient underwent US, TRUS, MRI and PET/CT examinations. In particular, prostate MRI represents the gold standard for the prostate evaluation since it provides a high soft tissue contrast resolution necessary to determine the site of origin of the tumour, its local extent, the presence of local adenopathy, aiding in planning surgical resection. The main imaging features on MRI examination are described in Table 2 (Yang et al., 2023).

The prostate MRI performed in our department revealed the presence of a voluminous heterogeneous mass in most sequences, indicating the presence of necrotic contextual areas. In particular, this was confirmed by the T1-w performed before and after contrasting medium administration. Necrosis and cystic change in these types of tumours are common, because of their high malignancy and rapid growth. The DWI and ADC sequences showed area of restricted diffusion, as expression of the

Table 1: Main role of each imaging modality

Imaging modality	Role	Advantages
TRUS	To provide an initial evaluation and detection of prostate abnormalities.	real-time images
CT	To evaluate lesion extension, lymph node involvement, and distant metastases.	detailed multiplanar images
MRI	To delineate tumour margins, assess local invasion, and detect lymph node metastases.	high soft tissue contrast
PET/CT	To detect distant metastases and assess treatment response.	To combine metabolic and anatomical imaging.

TRUS – transrectal ultrasound; CT – computed tomography; MRI – magnetic resonance imaging; PET/CT – positron emission tomography/CT

Table 2: Typical signal intensity of prostate sarcoma on magnetic resonance imaging sequences

MRI sequence	Signal intensity
T1-w	heterogeneous low signal mass
T2-w	heterogeneous intermediate to high signal mass
CE-T1	heterogenous contrast enhancement
DWI/ADC	mostly impeded diffusion, with high signal intensity at higher b values and low diffusion coefficient
Spectroscopy	marked increase in choline/citrate ratio

MRI – magnetic resonance imaging; DWI – diffusion weighted imaging; ADC – apparent diffusion coefficient

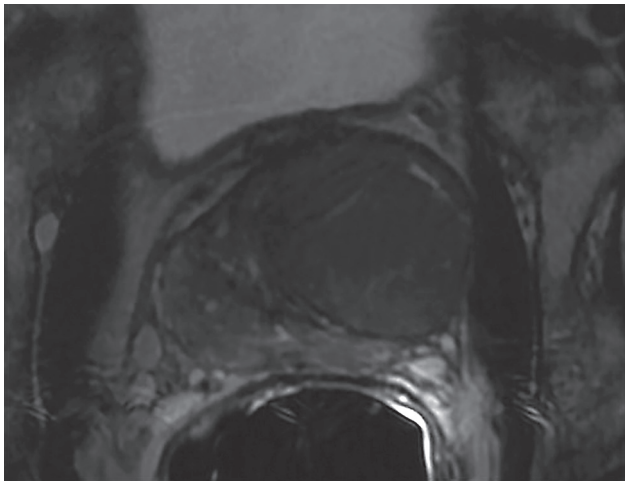

Figure 8: T2-w 1.5 magnetic resonance imaging of the prostate apex showed the presence of a capsule (low signal intensity complete line).

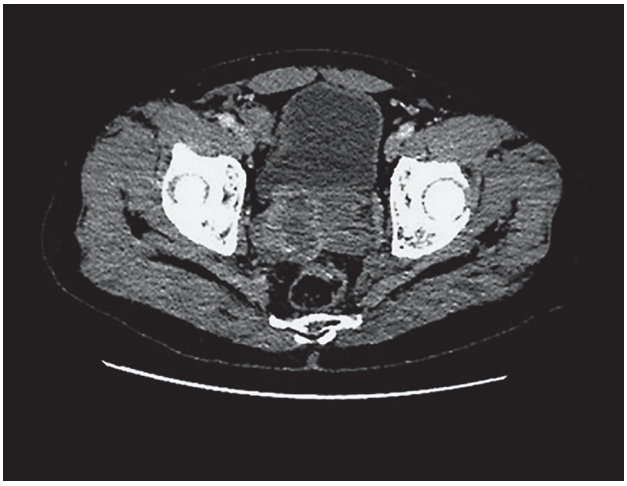

Figure 9: Axial computed tomography scan showed a prostate heterogeneous mass with hypodense areas suggesting contextual necrosis.

hyper cellularity of the prostate lesion. Spectroscopy generally shows a marked increase in the ratio of choline/citrate, according to the imaging features presented in this case (Wang et al., 2023; Nitta et al., 2024).

Imaging techniques play a key role also in staging prostate sarcoma, taking into account the size of the tumour, the extent of invasion, lymph node involvement and the presence of distant metastases at sites such as bone, lung, or liver. It is important to assess local invasion, as prostate sarcoma tends to invade surrounding structures, such as seminal vesicles, bladder, or rectum, indicative of locally advanced disease. Given the usual large size of the pelvic mass at the time of detection, it is important to distinguish its prostatic origin from the bladder which may be mistakenly considered the origin. In the reported case, the tumour was responsible for a mass effect on the surrounding structures, in particular on the bladder, and the presence of a complete pseudo-capsule was decisive in excluding the involvement of the perilesional tissue (Jaouani et al., 2023) (Figure 8).

The patient underwent a total-body PET/CT to detect distant metastases, such as pulmonary. Prostate sarcoma did not present CT features able to characterize the neoplasm. However, it confirmed the

Table 3: Main differences between prostate sarcoma and prostate adenocarcinoma

Feature	Prostate sarcoma	Prostate adenocarcinoma
Epidemiology	before 50 years old	after 50 years old
PSA level	normal	increased
Tissue/zone involved	mesenchymal tissue, in and around the prostate	glandular tissue, almost of the peripheral zone
Local invasion	common	rare at diagnosis
Metastasis	lung and liver; osteolytic bone lesion	osteoblastic bone lesion

PSA – prostate-specific antigen

Prague Medical Report / Vol. 126 (2025) No. 2, p. 96–102

presence of a large prostate mass with heterogeneous attenuation for the presence of necrosis/cystic areas and heterogeneous enhancement (Andreou et al., 2013) (Figure 9).

In the differential diagnosis it is important to distinguish prostatic sarcoma from prostate adenocarcinoma, as they are characterized by different management and prognosis. Imaging features can be helpful in differentiating, considering the zone involved, the presence and type of local invasion/metastases. In particular, the prostate adenocarcinoma arises in the glandular peripheral zone, while the prostate sarcoma was evident in the central zone. In addition to these differences, it should be considered the epidemiology, and the serum PSA value which is usually normal in prostate sarcoma due to the non-epithelial origin of the sarcomatous tumour (Rojas-Jiménez et al., 2013) (Table 3).

In the reported case, as confirmed by histology which represent any case the definite diagnosis, the main features were compatible with a prostate sarcoma.

Conclusion

Prostate sarcomas pose significant diagnostic challenges due to their rarity, heterogeneity, and propensity for rapid progression. Knowing the imaging features of prostate sarcoma may assist in the characterization of a prostate lesion and in the differential diagnosis with adenocarcinoma. Tumour invasion may be difficult to assess accurately without high-quality imaging, and it is essential to avoid misinterpreting these areas of mass effect as infiltration. Multidisciplinary collaboration among urologists, oncologists, and radiologists is essential to optimize patient management and improve clinical outcomes.

References

Andreou, A., Whitten, C., MacVicar, D., Fisher, C., Sohaib, A. (2013) Imaging appearance of sarcomas of the prostate. *Cancer Imaging* **13(2)**, 228–237.

Arham, A. B., Robinson, R. A., Chakra, M. A., O'Donnell, M. A. (2024) Leiomyosarcoma of the prostate: A novel approach to treatment – Case report and review of the literature. *J. Surg. Case Rep*. **2024(3)**, rjae138.

Ehat, N. T., Chuong, L., Dickman, J., Deng, T., Chang, G., Hwang, J. (2023) Prostate sarcoma. *IJU Case Rep*. **6(3)**, 165–168.

Girling, J., Whitaker, H., Mills, I., Neal, D. (2007) Pathogenesis of prostate cancer and hormone refractory prostate cancer. *Indian J. Urol*. **23(1)**, 35.

Hodotsuka, N., Suzuki, Y., Suzuki, K., Honda, Y., Endo, S., Kuribayashi, E., Obayashi, K., Minowa, T., Hatori, T., Kondo, Y. (2023) A case of complete resection of prostate stromal sarcoma after neoadjuvant chemotherapy. *IJU Case Rep*. **6(4)**, 239–243.

Jaouani, L., Zaimi, A., Al Jarroudi, O., Brahmi, S. A., Afqir, S. (2023) Undifferentiated sarcoma: A rare tumor of the prostate. *Cureus* **15(6)**, e41056.

Luo, C., Liu, L., Zhang, G. (2024) Secondary myeloid sarcoma in the prostate: A case report. *Asian J. Surg*. **47(3)**, 1636–1638.

Nitta, S., Kandori, S., Kojo, K., Suzuki, S., Hamada, K., Chihara, I., Shiga, M., Sakka, S., Nagumo, Y., Kimura, T., Mathis, B. J., Negoro, H., Okuyama, A., Higashi, T., Nishiyama, H. (2024) Adult genitourinary sarcoma: Analysis using hospital-based cancer registry data in Japan. *BMC Cancer* **24(1)**, 215.

Phuong, V. T., My Hanh, B. T., Hang, N. T., Thanh, T. D., Lieu, D. Q., Duc, N. M. (2023) Prostatic stromal sarcoma: A case report and literature review. *Radiol. Case Rep*. **18(9)**, 2918–2923.

Qin, E. S., Richards, B., Smith, S. R. (2023) Function in cancer patients: Disease and clinical determinants. *Cancers* **15(13)**, 3515.

Rojas-Jiménez, A., Otero-García, M., Mateos-Martin, A. (2013) Stromal prostatic sarcoma: A rare tumor with rare clinical and imaging presentation. *J. Radiol. Case Rep*. **7(7)**, 24–31.

Wang, F. F., Zhang, X. N., Wang, X. J. (2023) Magnetic resonance imaging analysis of embryonal rhabdomyosarcoma of the prostate. *Technol. Health Care* **31(6)**, 2243–2250.

Yang, B., Yuan, J., Yu, S., Wang, D. (2023) A case report of primary mesenchymal sarcoma of the prostate and the thoughts on its treatment. *Asian J. Surg*. **46(11)**, 4934–4935.